SAGE-Hindawi Access to Research
International Journal of Electrochemistry
Volume 2011, Article ID 434186, 7 pages
doi:10.4061/2011/434186

Research Article

A Graphite Oxide Paper Polymer Electrolyte for Direct Methanol Fuel Cells

Ravi Kumar, Mohamed Mamlouk, and Keith Scott

School of Chemical Engineering and Advanced Materials, Newcastle University, Newcastle upon Tyne NE1 7RU, UK

Correspondence should be addressed to Keith Scott, k.scott@ncl.ac.uk

Received 14 June 2011; Revised 12 August 2011; Accepted 12 August 2011

Academic Editor: Jiujun Zhang

A flow directed assembly of graphite oxide solution was used in the formation of free-standing graphene oxide paper of approximate thickness of 100 μm. The GO papers were characterised by XRD and SEM. Electrochemical characterization of the GO paper membrane electrode assembly revealed proton conductivities of 4.1×10^{-2} S cm^{-1} to 8.2×10^{-2} S cm^{-1} at temperatures of 25–90°C. A direct methanol fuel cell, at 60°C, gave a peak power density of 8 mW cm^{-2} at a current density of 35 mA cm^{-2}.

1. Introduction

Polymer electrolyte fuel cells (PEMFCs) have been projected as promising power sources for many potential applications [1]. The present PEMFCs research is based on polymer electrolyte membranes which provide appropriate fuel cell performance in terms of conductivity, chemical, mechanical stability, durability, and fuel crossover [2, 3]. Perfluorinated sulphonic acids (PFSA-)- based membranes are widely used as these membranes show good conductivities in the range of 0.01 to 0.1 S cm^{-1} in a humid environment. However unsatisfactory durability and reliability of these membranes hinders the successful commercialization of fuel cells. To improve the performance of polymer electrolyte fuel cells and replace the cell components like membranes, different approaches have been employed: (1) development of Nafion-based composite membranes to increase the conductivity, mechanical strength, and chemical stability [4]: (2) direct use of functionalized materials like fullerene for polymer electrolyte fuel cells and PVDF mixed fullerene for direct methanol fuel cells [5, 6].

The preparation and characterization of graphene oxide paper was reported by Ruoff et al. [7], and they believed that these materials can be adopted for applications including molecular storage, ion conductors and super capacitors. The mechanism of proton conductivity in solids, is based on two methods; one is the vehicular model, where formation of an ion adduct with carrier molecule occurs—if it is water then protons form hydronium ions. In a non-vehicular model hopping of protons occurs from site to site without carrier molecules. The activation energy of proton conduction depends on the distance between the hopping sites; if the distance is short, for example 0.24–0.25 nm, in case of two oxygen atoms, then proton conduction is free from kinetic activation [8, 9].

Hydration of GO incorporates the water molecule between GO sheets which presumably form hydrogen bonds [7]. Scanning tunnelling microscopy shows oxygen atoms on GO are arranged in a rectangular pattern with a lattice constant of 0.27 nm × 0.41 nm [10]. Based on this information, GO presumably shows both types of conduction mechanism; with hopping of protons via oxygen atoms present on basal planes and edges, and with a vehicular mechanism, where, due to the presence water molecule between layers, protons might form hydronium ions. On the contrary, carbon based materials like fullerenol $C_{60}(OH)_n$ have reported conductivities of 7×10^{-6} S cm^{-1} with no significant proton conductivity for fuel cell application. Therefore GO is potentially interesting for use as polymer electrolytes in PEMFCs [11]. In the present paper, we report the characterization and use of

a free standing GO paper membrane as a polymer electrolyte membrane for PEMFCs using methanol.

2. Experimental Section

2.1. Synthesis of Graphite Oxide and Graphene Oxide Paper. Graphite oxide was synthesized from natural flake graphite by the modified Hummers method [12]. In brief, 200 mg of Graphite particles were immersed in concentrated sulfuric acid (46 mL), and $KMnO_4$ (6 g) was added slowly in small quantities in which temperature was maintained between the 0 and 5°C using an ice bath, After the complete oxidation of $KMnO_4$, the mixture was heated to 37°C and kept at this temperature about 30 min. Then 12 mL of distilled water is added slowly to this mixture then temperature of mixture is raised to 95°C, and it is maintained for about 15 min. This mixture was further diluted with 280 mL of water, and later 20 mL of 30% H_2O_2 was added and left for 5 min, then solid was filtered off and washed with 5% HCl until filtrate was free from sulphate ions. GO thus obtained was further washed thoroughly with water and dried in air for 24 hours.

Colloidal solutions of graphite oxide was prepared in water at a concentration of 2 mg cm^{-3}(mg/mL) using an ultrasonic water bath. Free-standing graphene oxide paper was made by filtration of the resulting colloid through a membrane filter (cellulose acetate membrane filter of 47 mm in diameter, 0.2 μm pore size) followed by air drying and peeling off from the filter.

2.2. Membrane Electrode Assembly and Fuel Cell Fabrication. To prepare the fuel cell membrane electrode assemblies, as-prepared free-standing GO paper (without any binder) was sandwiched between a Pt-Ru/C (20% Pt, 10% Ru) of 1 mg cm^{-2} anode and a Pt/C (20%) of 1 mg cm^{-2} (from Johnson Mathey Corp.) cathode. The catalyst ink was made by ultrasonicating with 2-propanol and 15% Nafion ionomer, and the ink was sprayed onto Toray carbon paper. The MEA was hot pressed at 135°C and a pressure of 60 kg cm^{-2} for 3 minutes and used for fuel cell polarization and proton conductivity studies. The MEA was set between two high-density graphite blocks impregnated with phenolic resin, and the active electrode area (1 cm^2) was formed by the parallel gas flow channels area. Electric cartridge heaters were mounted at the rear of the graphite blocks to maintain the desired temperature, which was monitored by imbedded thermocouples and controlled with a temperature controller. Gold-plated steel bolts were screwed into the blocks to allow electrical contact. Fuel cell polarizations were carried out by using ACM instruments.

2.3. Fuel Crossover. Methanol permeability was measured using a liquid diffusion cell composed of two compartments. One compartment (A) was filled with a 10 M methanol/water solution, and the other compartment (B) was filled with deionised water. The membrane (4.9 cm^2) was placed between the two compartment, and both the solutions were stirred continuously during experiments. The methanol concentrations were obtained by measuring the refractive index for 0.1 mL sample from each compartment at fixed time intervals. The methanol permeability (P) was calculated by the following equation:

$$P(\mathrm{cm^2\,s^{-1}}) = k \times V_{\mathrm{B}} \times \frac{L}{A} \times C_A, \tag{1}$$

where k is the slope of the straight line plot of methanol concentration in solution B versus permeation time (mol s^{-1}); V_{B} is the volume of solution B (mL); C_A is the concentration of methanol in the A cell (mol L^{-1}); A is the membrane area (cm^2); L is the membrane thickness (cm).

Oxygen crossover of GO paper was measured by using bubble gauge method [13]. A mass flow meter (5 to 90 cm^{-3} min^{-1}) was used to measure the crossover flow before and after fuel cell polarization. A gas phase pressure was imposed on cathode to increase the crossover flow. The inlet on the nonpressurised side was closed and a flow meter on the nonpressurised side is used to measure the outgoing flow rate.

2.4. Instruments. X-ray diffraction experiment was performed using a Rigaku diffractometer (CuKα radiation, X-ray wavelength $\lambda = 1.5406$ Å, operating at 40 keV). Fourier transform infrared spectroscopy (FTIR) was measured on Varian 800 FT-IR spectrometer system with wave number between 4000 and 500 cm^{-1}. Scanning electron microscopy (SEM) was made using a HITACHI S-4700 (Japan) machine. Methanol permeability of the membrane was measured by using refractive index detector (Refracto 30P (Japan)).

AC impedance measurements were performed to measure the proton conductivity using a ZAHNER Elektrik impedance measurement unit over a frequency range of 100 KHz–100 mHz. The impedance cell was operated at 100% RH at ambient pressure and with a variable temperature. The thermal stability of the graphene oxide paper was measured by thermo-gravimetric analysis using a STA409PC machine (NETZSCH-Gerätebau GmbH Germany) over a temperature range of 25–650°C with a scan rate of 5°C min^{-1} under nitrogen flow (50 mL min^{-1}). Fuel cell polarizations were measured by using Ministat potentiastat (sycopel scientific Ltd.)

3. Results and Discussion

Figures 1(a) and 1(b) show the XRD spectra of graphite oxide and graphite powder. The peak observed at 26.45° in the graphite sample corresponds to the interplanar distance between the different graphene layers. Chemical oxidation of graphite disturbs ordering of layer and introduces a variety of functional groups (epoxide, carboxyl, etc.) as the C–C bonds are broken during the oxidation process [14]. The functional groups increase the interplanar distance between the sheets. This larger distance between graphene oxide sheets shifts the XRD peak to smaller angles, thus the appearance of broader peak at around 11.26°.

FTIR studies confirmed the successful oxidation of graphite to graphite oxide, as shown in Figure 2. The presence of different types of oxygen functionalities in GO at

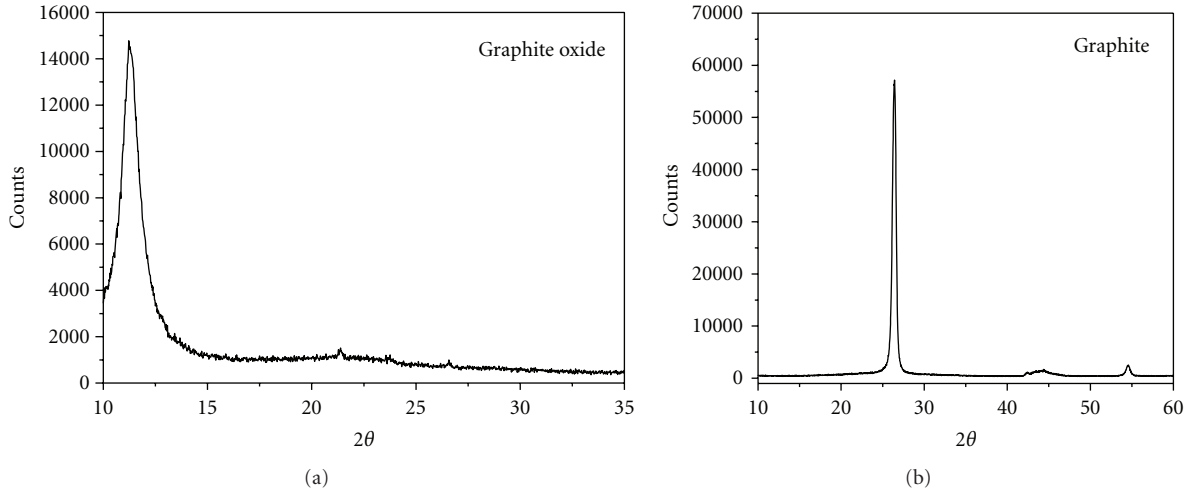

Figure 1: X-ray spectrum of graphite oxide (a), graphite powder (b).

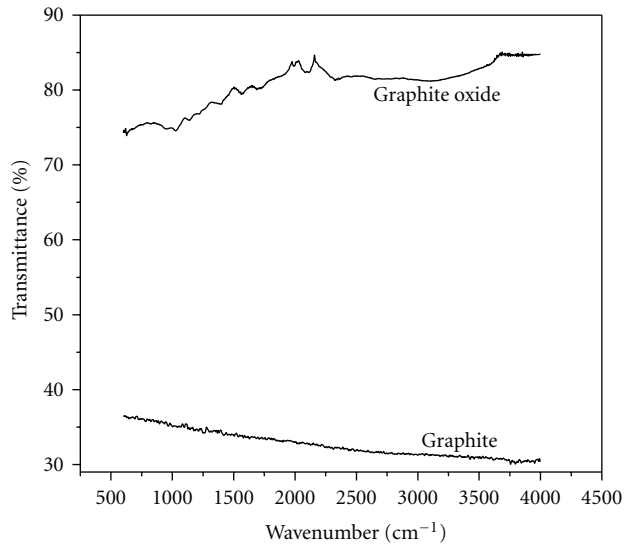

Figure 2: FTIR spectra of graphite and graphite oxide.

1800–2200 cm^{-1} (O–H stretching vibrations) and at 1400–1600 cm^{-1} (stretching vibrations from C=O), while no significant peak was found in graphite. These results depict OH and other functionalities, such as COOH groups, in the resultant GO, which also confirmed the successful oxidation of graphite.

The fracture edges of GO paper was imaged via scanning electron microscopy shown in Figure 3(a), which revealed the stacking of less densely packed thin wavy layers through the cross section with a thickness of layers of approximately 100–200 nm thick. Cross section of MEA made with GO paper is shown in Figure 3(b), where a notable morphology change can be observed. Higher magnification (15000xs) of cross section of GO paper in MEA shows a complete deterioration of layer structure due to disintegration of GO paper, shown in Figure 3(c). Moreover, a significant disintegration of the GO paper results in detachment of catalytic layer which can be seen in cross section of MEA (Figure 3(b)). Surface morphology of GO paper removed from the MEA (Figure 4(b)) shows increased roughness, while the fresh one shows smooth surface (Figure 4(a)).

Mechanism for the formation of GO paper was reported by Ruoff et al. [7], (Nature 448 (2007) 457) by vacuum filtration. During this stage, the sheets are more likely to be aligned on top of each other in the ever-growing deposit and are probably also smoothed out by the water flow. After drying, if water is poured on top of the GO paper, the paper swells sufficiently to allow the water to seep through, and then returns back to the dry state. A piece of graphite oxide paper left in water for several hours does not disperse and maintains its shape, but disintegrates easily if it is handled while still wet. If a wetted graphite oxide paper is left to dry, it will regain its mechanical integrity and can again be handled without failure. This mechanism clearly states that binder less GO paper under liquid fuel conditions mechanically disintegrates and also due to pressurised fuel gases disrupts the GO paper.

The ionic conductivity was measured by AC impedance spectroscopy (through plane) from membrane electrode assembly fabricated with GO paper membrane. The resistance associated with the membrane at zero phase angle was used to estimate the proton conductivity of the membrane using the equation, $\sigma = (1/R)(L/A)$, where R is the bulk resistance of the membrane, L represents the membrane thickness, and A the membrane area. The conductivity of the MEA was 4.1×10^{-2} S cm^{-1} at 298 k and increased with temperature at 363 K to 8.2×10^{-2} S cm^{-1}. Figure 5 shows the plot of $1/T$ versus log of conductivity which follows an Arrhenius behavior with activation energy of 0.83 eV. High proton conductivity of graphite oxide membrane may be attributed to a Grotthus type mechanism, in which reorganization of hydrogen bonds play a vital role in the presence of water between each layer. Bridging oxygen atoms in GO structure as epoxy oxygen, in a rectangular fashion, leads to vehicular mode of proton transportation. The lower in activation energy is an evidence for high ionic conductivity,

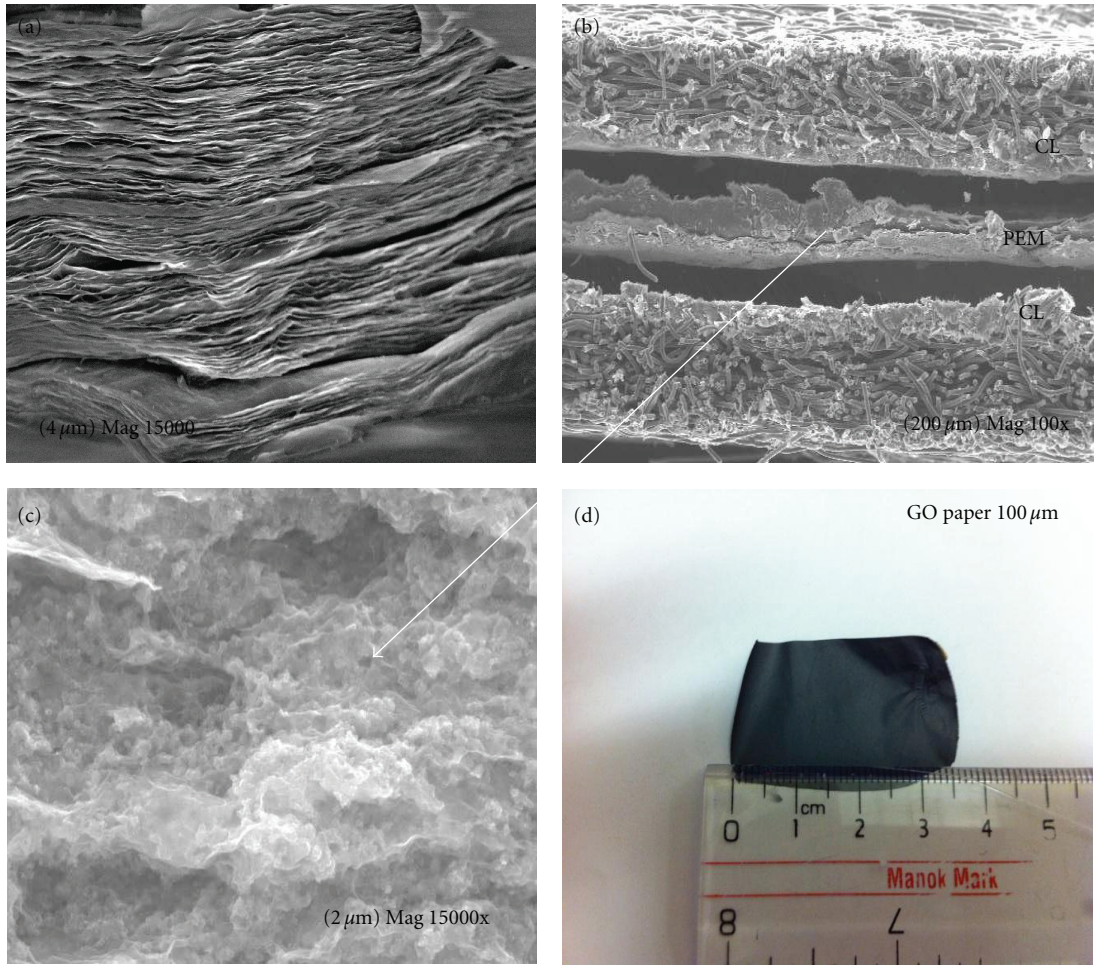

Figure 3: SEM images of Graphite oxide paper and MEAs made with GO paper. (a) Cross section of GO paper, (b) cross section of GO paper within the MEA, (c) cross section of GO paper in the MEA, and (d) picture of GO paper.

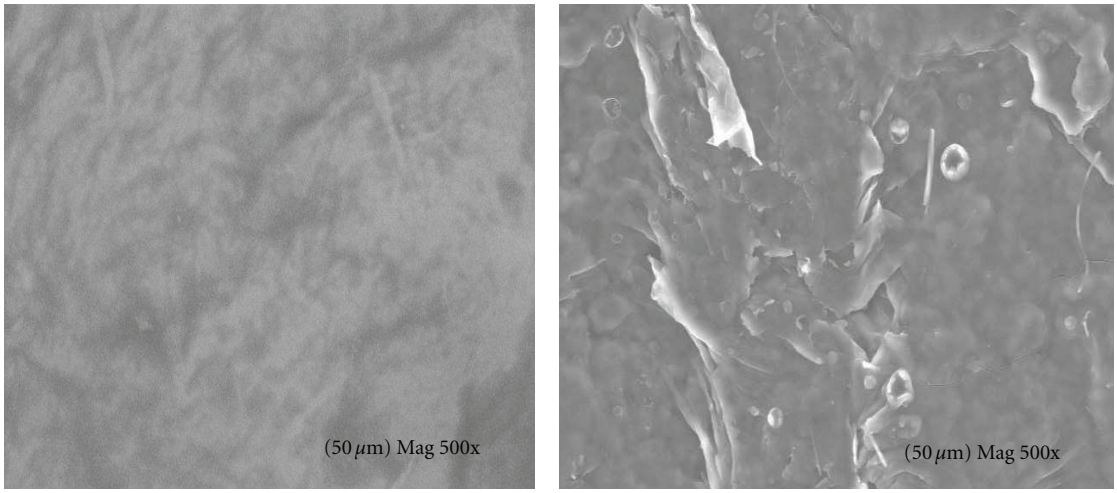

(a) (b)

Figure 4: SEM images of surface morphology of Graphite oxide paper. (a) Surface of fresh GO paper. (b) Surface of GO paper removed from MEA after polarization.

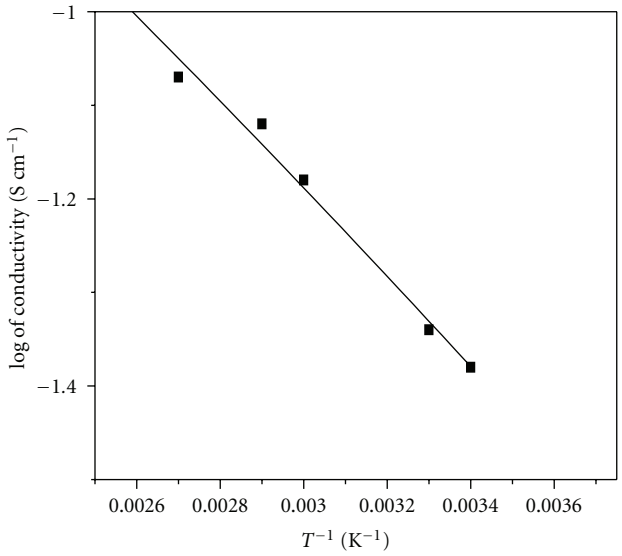

Figure 5: Temperature-dependent proton conductivity of graphite oxide membrane.

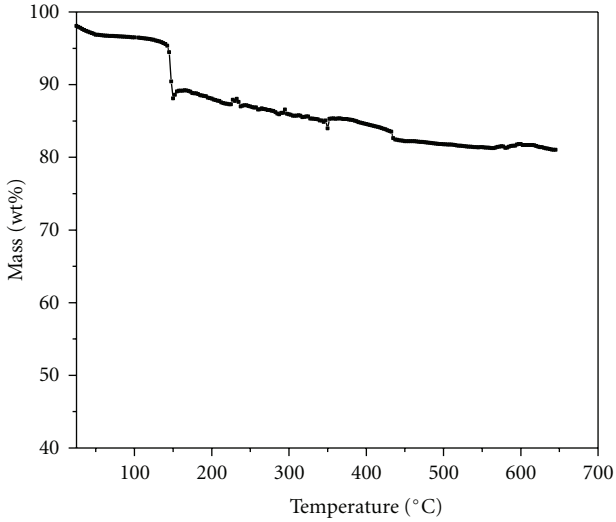

Figure 6: Thermogravimetric analysis of graphite oxide membrane over a temperature range of 25 to 650°C.

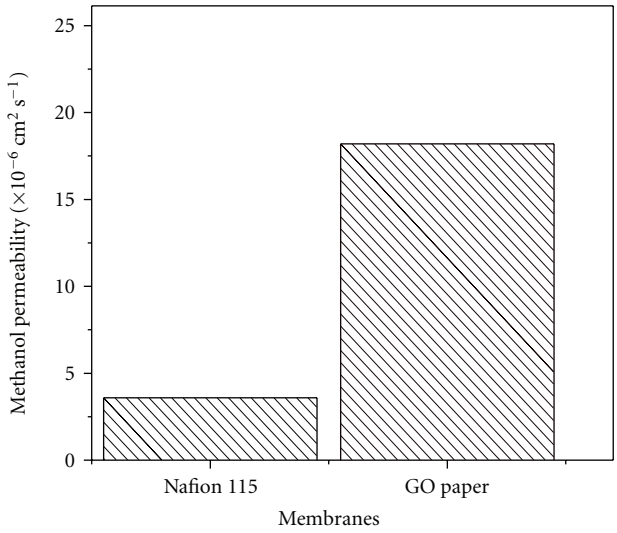

Figure 7: Methanol permeability of Nafion 115 and Graphite oxide paper.

which is attributed to the arrangement of oxygen atoms in rectangular fashion with a lattice constant of 0.27 nm × 0.41 nm [10].

Thermal analysis of GO paper membrane from 25°C to 650°C under nitrogen flow is shown in Figure 6; the rapid expansion of graphite oxide occurred at 149°C [7]. Mechanical properties of graphene oxide paper strongly depend on its water content, as the moisture content of graphite oxide paper decreases with increasing temperature. The significant mass loss (12 wt%) occurred during sample heating from 25°C to 149°C. Above this temperature, there was an almost constant mass throughout the temperature, range up to 650°C, which supports the increasing conductivity with increased temperature.

Figure 7 shows the methanol permeability of Nafion 115 and GO paper. The GO paper has much higher methanol permeability of 18.2×10^{-6} cm^2 s^{-1} than Nafion 115 which has methanol permeability of 3.36×10^{-6} cm^2 s^{-1}. The measured methanol permeability for Nafion 115 membrane is in good agreement with the literature [15, 16]. Though, high proton conductivity and low methanol permeability are important properties for proton exchange membranes in DMFCs, GO paper shows good proton conductivity. The GO paper swells sufficiently to allow the water to seep through [7], therefore observed methanol permeability of GO is increased.

Figure 8(a) shows the single cell DMFC polarization data using a graphite oxide paper membrane. The cell was equilibrated by feeding a 1.0 M methanol solution to the anode for 24 hours. The single cell performances of MEAs based on GO paper and Nafion 115 membranes, measured at 60°C under feed flow rates of 3 cc min^{-1} of methanol and 400 cc min^{-1} oxygen at atmospheric pressure. The open-circuit voltage (OCV) was 0.7 V at 60°C. This data indicates that due to the easy hydration of the graphite oxide paper, methanol crossover was significant, resulting in a mixed potential at the cathode which reduced the OCV to the detriment of the DMFC performance. The DMFC gave a peak power density of 8 mW cm^{-2} at a current density of 35 mA cm^{-2}, whereas single cell polarization of standard membrane Nafion 115 gave power density of 62 mW cm^{-2} at a current density of 97 mA cm^{-2} shown in Figure 8(b) (Nafion 115 has approximate comparable thickness of 120 μm to GO paper 100 μm), which was tested as a reference under the same experimental conditions.

After 24 hours, equilibration fuel cell polarisations were performed, up to fifth polarisation, MEA was stable and results are reproducible. At Sixth polarisation, the OCV was reduced to 0.550 V and cell performance was dropped to 3 mW cm^{-2}. Then the OCV drops to 0 V because the mechanical stresses of the flow fields or sealing edges tear

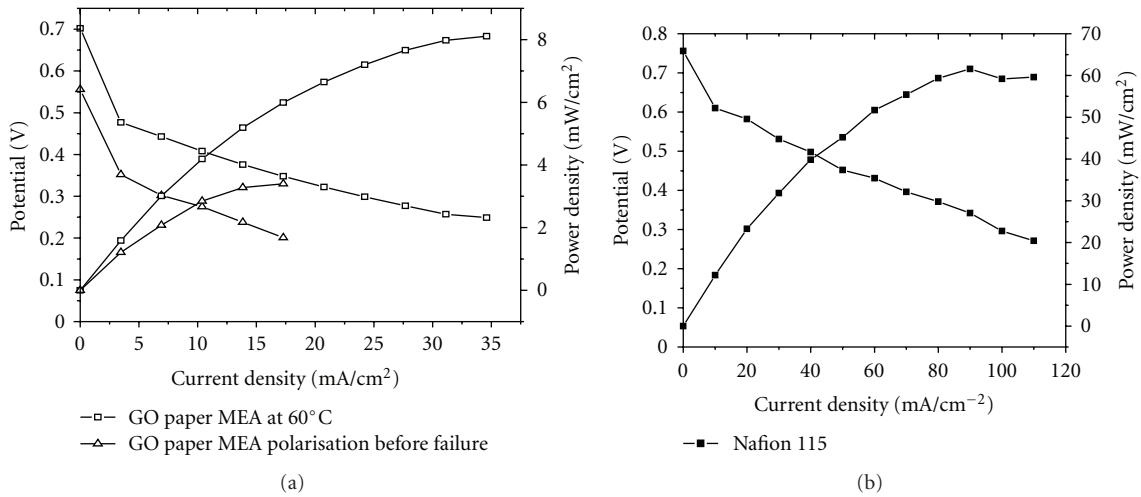

FIGURE 8: (a) Polarization curves of GO paper MEA at scan rate of 5 mV s^{-1} for direct methanol fuel cell 1 M methanol (flow rate 3 cc min^{-1}) and oxygen (flow rate 400 cc min^{-1}) at 60°C. (b) Polarization curves of Nafion 115 MEA at 5 mV s^{-1} for direct methanol fuel cell 1 M methanol (flow rate 3 cc min^{-1}) and oxygen (flow rate 400 cc min^{-1}) at 60°C.

the swelled GO paper (without any binder) and also the oxygen flow at the cathode mechanically accelerated the disintegration of GO paper, resulting in oxygen flow (the measured oxygen flow was 6 cc min^{-1}, which confirms the tearing of membrane) to the anode side and increased air bubbles in methanol outlet. The oxygen crossover of fresh MEA under dry state was studied, and no significant gas crossover was observed. Three MEAs were prepared and tested for reproducibility, and their fuel cell performances are almost the same for all the MEAs before failure.

The estimated conductivity from the IR region of the polarization curve is ca 1.4×10^{-2} S cm^{-1}. The difference in conductivity measured by AC impedance was probably due to disintegration of graphene oxide sheets, due to prolonged exposure to water [6]. Overall the fuel cell performance was poor and in order to overcome this, the graphene oxide membrane material could be used as a composite in a suitable polymer matrix, such as Nafion or polyvinyl alcohol. Our future work will prepare the graphite oxide composite membrane with binder to improve the strength and flexibility of membrane that can reduce the methanol crossover.

4. Conclusions

Fuel cell membranes using graphite oxide have been prepared and characterized and used in a DMFC. The ionic conductivity of graphite oxide paper membrane was high and thus suitable for methanol fuel cells. From the membranes proton conductivity and activation energy, the transport mechanism is due to the presence of acidic functional groups and intermolecular hydrogen bonding, and also oxygen atoms percolate close to each other on a molecular plane making abundant proton conducting paths. However although the conductivity was high, the fuel cell performance was poor. Understanding and utilizing this structure in developing new composite membranes may provide membranes for the DMFC that can operate in wide range of temperature.

Acknowledgment

The authors thank EPSRC for supporting this work through the SUPERGEN fuel cell consortium.

References

[1] J. Wu, X. Z. Yuan, J. J. Martin et al., "A review of PEM fuel cell durability: degradation mechanisms and mitigation strategies," *Journal of Power Sources*, vol. 184, no. 1, pp. 104–119, 2008.

[2] K. Kleiner, "Assault on batteries," *Nature*, vol. 441, pp. 1046–1047, 2006.

[3] J. P. I. de Souza, S. L. Queiroz, K. Bergamaski, E. R. Gonzalez, and F. C. Nart, "Electro-oxidation of ethanol on Pt, Rh, and PtRh electrodes: a study using DEMS and in-situ FTIR techniques," *Journal of Physical Chemistry B*, vol. 106, no. 38, pp. 9825–9830, 2002.

[4] R. Kannan, B. A. Kakade, and V. K. Pillai, "Polymer electrolyte fuel cells using nafion-based composite membranes with functionalized carbon nanotubes," *Angewandte Chemie—International Edition*, vol. 47, no. 14, pp. 2653–2656, 2008.

[5] K. Tasakia, A. Venkatesana, P. Pugazhendhib, and R. O. Loutfyb, "Fullerene composite proton conducting membranes for polymer electrolyte fuel cells operating under low humidity conditions," *Preprint Papers–American Chemical Society, Division of Fuel Chemistry*, vol. 49, no. 2, p. 530, 2004.

[6] T. Hirakimoto, K. Fukushima, Y. Li, S. Takizawa, K. Hinokuma, and T. Senoo, Advanced Materials Laboratories, Sony Corporation 4-16-1 Okata Atsugi-shi, Kanagawa, 243-0021, Japan.

[7] D. A. Dikin, S. Stankovich, E. J. Zimney et al., "Preparation and characterization of graphene oxide paper," *Nature*, vol. 448, no. 7152, pp. 457–460, 2007.

[8] K. D. Kreur, "Proton conductivity: materials and applications," *Chemistry of Materials*, vol. 8, p. 610, 1996.

[9] T. Norby, "Solid-state protonic conductors: principles, properties, progress and prospects," *Solid State Ionics*, vol. 125, no. 1, pp. 1–11, 1999.

[10] D. Pandey, R. Reifenberger, and R. Piner, "Scanning probe microscopy study of exfoliated oxidized graphene sheets," *Surface Science*, vol. 602, no. 9, pp. 1607–1613, 2008.

[11] K. Hinokuma and M. Ata, "Fullerene proton conductors," *Chemical Physics Letters*, vol. 341, no. 5-6, pp. 442–446, 2001.

[12] W. S. Hummers Jr. and R. E. Offeman, "Preparation of graphitic oxide," *Journal of the American Chemical Society*, vol. 80, no. 6, p. 1339, 1958.

[13] M. M. Mench, "Transport in fuel cell systems," in *Fuel Cell Engine*, p. 191, Wiley John & Sons, New York, NY, USA, 2007.

[14] B. Segar and P. V. Kamath, "Electrocatalytically active graphene-platinum nanocomposites. role of 2-D carbon support in pem fuel cells," *Journal of Physical Chemistry C*, vol. 113, no. 19, pp. 7990–7995, 2009.

[15] J. Sauk, J. Byun, and H. Kim, "Composite nafion/polyphenylene oxide (PPO) membranes with phosphomolybdic acid (PMA) for direct methanol fuel cells," *Journal of Power Sources*, vol. 143, no. 1-2, pp. 136–141, 2005.

[16] V. Baglio, A. Stassi, F. V. Matera, A. Di Blasi, V. Antonucci, and A. S. Arico, "Optimization of properties and operating parameters of a passive DMFC mini-stack at ambient temperature," *Journal of Power Sources*, vol. 180, no. 2, pp. 797–802, 2008.